Journal of Engineering Mathematics (2005) 52: 337–353
DOI 10.1007/s10665-005-2732-6


# Convective and absolute instability in the incompressible boundary layer on a rotating disk in the presence of a uniform magnetic field

H.A. JASMINE and J.S.B. GAJJAR
*School of Mathematics, University of Manchester, Booth Street, M13 9PL, U.K (gajjar@manchester.ac.uk)*

Received 8 September 2003; accepted in revised form 21 February 2005

**Abstract.** The stability of a conducting fluid flow over a rotating disk with a uniform magnetic field applied normal to the disk, is investigated. It is assumed that the magnetic field is unaffected by the motion of the fluid. The mean flow and linear stability equations are solved for a range of magnetic field-strength parameters and the absolute/convective nature of the stability is investigated. It is found that increasing the magnetic field parameter is in general stabilizing.

**Key words:** absolute/convective stability, hydrodynamic-stability theory, magneto-hydrodynamics, rotating-disk flow

## 1. Introduction

The flow over a rotating disk in a non-conducting fluid has been extensively studied in the literature. One reason for this is that the Von-Kármán [1] self-similar solution for the flow over a rotating disk is one of the few exact solutions of the Navier-Stokes equations for a fully three-dimensional boundary-layer flow. It is thus argued that the stability characteristics of this flow, and in particular cross-flow instability, will have some similarities with the stability of other fully three-dimensional boundary-layer flows which arise in the important aerodynamic context.

Rotating fluid flows in the presence of a magnetic fields are important in many industrial applications such as electromagnetic stirring of liquid metals. Pao [2] was one of the first to investigate the flow of an incompressible viscous conducting fluid over a rotating disk when a circular magnetic field is imposed. He concludes that the presence of the magnetic field thickens the flow boundary layer and also reduces the strength of the axial flowfield. Furthermore, for sufficiently large values of the applied magnetic field, the boundary layer separates from the surface of the disk.

In the current paper we consider rotating-disk flow but in a conducting fluid in the presence of a magnetic field applied normal to the disk. The main aims of the work are to investigate the stability of this flow. This problem, without the presence of a magnetic field, has been studied in detail by *inter alia* Lingwood [3], who presents results on absolute instabilities, Turkyilmazoglu *et al.* [4] where compressibility effects are addressed, and Turkyilmazoglu and Gajjar [5], where results for both convective and absolute instabilities for incompressible flows are discussed. In [3], and [6], it is shown that double-pole-type singularities of the dispersion relationship also exist at much lower Reynolds numbers than that required for the flow to be absolutely unstable. Lingwood [7] has also conducted a series of experiments where it is claimed that the Reynolds number for the flow to become transitional in her experiments is very close to the critical Reynolds number delinineating regions of absolute and convective instabilities calculated from linear stabilty theory. However, the suggestion of a global absolutely unstable mode is not supported

by numerical simulations of the full linearized Navier-Stokes equations conducted by Davies and Carpenter [8]. Work by Pier [9] suggests that non-linear effects and secondary instability of the primary absolute instability may be responsible for the sharp transition front observed in Lingwood's experiments.

When a normal magnetic field is present, the mean flow velocities can be significantly affected as shown by Sparrow and Cess [10]. In their work, with the additional effects of heat transfer, it is found that the presence of a normal magnetic field significantly decreases the flow velocities in the boundary layer. In the current work the mean flow is essentially the same as in [10], but without heat-transfer effects. In deriving the mean flow we make use of similar assumptions namely that the the effects of the electric field are negligible and that the magnetic field is unaffected by the fluid motion. Thus, the main effect on the fluid flow is through the presence of an additional force term, the Lorentz force, in the momentum equations. These assumptions apply to situations with low magnetic Reynolds numbers where the magnetic field is dominated by diffusive as opposed to advection effects.

Making use of the above assumption, a self-similar form for the mean flow can be obtained. By making use of the parallel-flow approximation the linear stability equations are derived. These equations are then solved numerically by using a spectral method with arclength continuation. The branch points where the group velocity $\frac{\partial \omega}{\partial \alpha}$ tends to zero are searched for in the $\alpha$- and $\omega$-planes. The convective and absolute instability characteristics of the mean velocity profile are discussed. The numerical results show that the range of convective as well as absolute instability is significantly reduced as the strength of the magnetic field is increased.

This paper is organized as follows. In Sections 2.1 and 2.2, the general governing equations of the motion in the rotating frame and the basic flow equations are given. The linear stability theory is applied in Section 2.3 and the linear disturbance equations governing the viscous flow are given. The mean flow properties and the stability results are discussed in Sections 3 and 4.

## 2. Mathematical formulation

### 2.1. Governing equations of the flow

We consider the three-dimensional boundary-layer flow of an incompressible, electrically conducting viscous fluid on an infinite disk which rotates about its axis with a constant angular velocity $\Omega\mathbf{k}$. A uniform magnetic field $\mathbf{B} = B_0\mathbf{k}$ is applied to the system, where $\mathbf{k}$ is a unit vector parallel to the $z$-axis; see Figure 1.

In order to non-dimensionalize the Navier-Stokes equations, we introduce non-dimensional quantities $r^*, \theta^*, z^*, t^*, u^*, v^*, w^*$, $\mathbf{B}^*$, and $P^*$:

$$r = Lr^*, \quad z = Lz^*, \quad \theta = \theta^*, \quad t = \frac{L}{U_c}t^*, \quad P = \rho U_c^2 P^*,$$
$$u = U_c u^*, \quad v = U_c v^*, \quad w = U_c w^*, \quad \mathbf{B}^* = B_0\mathbf{B},$$

where $L$ is a given length scale, say a fixed radial location, and $U_c = L\Omega$ is a given velocity scale. For convenience of writing, we shall suppress the * over the non-dimensional variables.

Thus, relative to non-dimensional cylindrical polar coordinates $(r, \theta, z)$ which rotate with the disk, the full time-dependent, unsteady magnetohydrodynamic equations governing the viscous fluid flow are as follows:

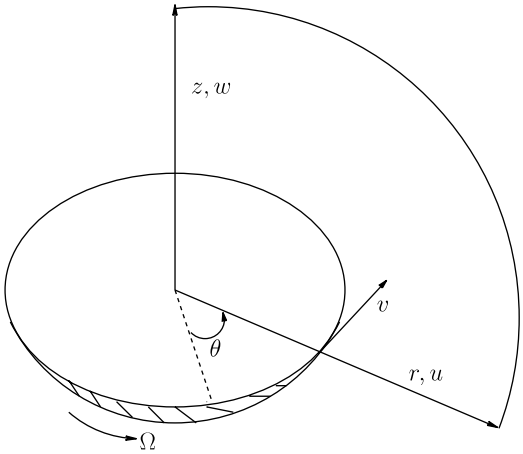


*Figure 1.* A schematic of the flow configuration showing the non-dimensional coordinates $(r, \theta, z)$ and corresponding velocities $(u, v, w)$.

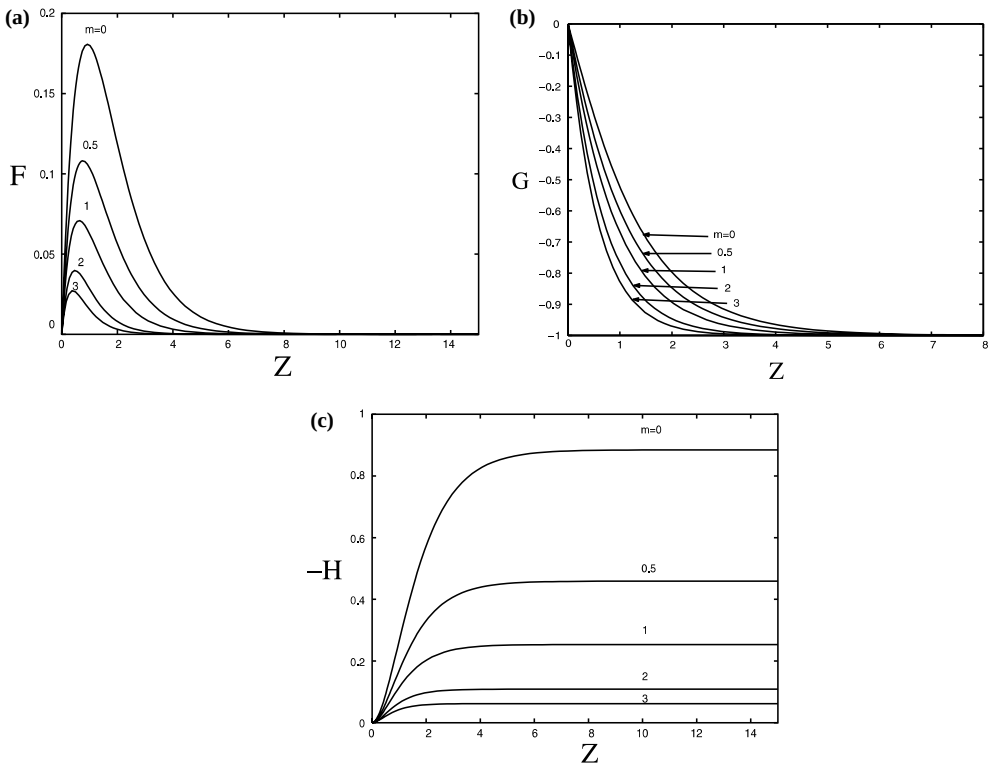


*Figure 2.* Plots of the similarity profiles: (a) crossflow velocity $F(Z)$, (b) azimuthal velocity $G(Z)$ and (c) normal velocity $H(Z)$ for different values of $m$.

$$\frac{\partial \mathbf{u}}{\partial t} + \mathbf{u}.\nabla\mathbf{u} + 2(\mathbf{k}\times\mathbf{u}) = -\nabla(P - \frac{1}{2}(\mathbf{k}\times\mathbf{r})^2) + m\mathbf{J}\times\mathbf{B} + \frac{1}{\mathrm{Re}}\nabla^2\mathbf{u}, \tag{1a}$$

$$\frac{\partial \mathbf{B}}{\partial t} = \nabla\times(\mathbf{u}\times\mathbf{B}) + \frac{1}{\mathrm{Re}_m}\nabla^2\mathbf{B}, \tag{1b}$$

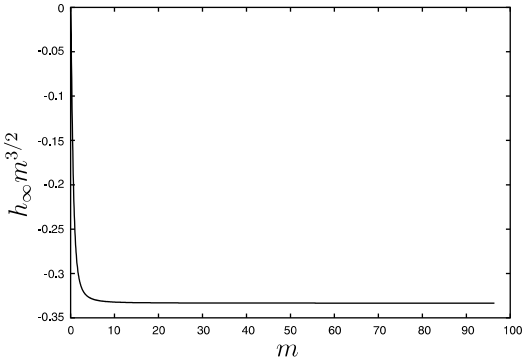


*Figure 3.* Magnetic-field strength $m$ *vs.* $h_\infty m^{\frac{3}{2}}$.

together with

$$\nabla.\mathbf{J}=0, \quad \nabla\times\mathbf{E}=-\frac{\partial\mathbf{B}}{\partial t}, \quad \nabla.\mathbf{B}=0, \tag{1c}$$

and

$$\mathbf{J}=\mathbf{E}+\mathbf{u}\times\mathbf{B}$$

is the current density. Here $m=\sigma B_0^2/(\rho\Omega)$ is the magnetic interaction parameter, $\mathrm{Re}=\Omega^2 L/\nu$ is the Reynolds number, $\mathrm{Re}_m=\sigma\mu_0 L^2\Omega$ is the magnetic Reynolds number, $\mu_0$ is the magnetic permeability (which we can take to that of free space), $\sigma$ is the electrical conductivity of the fluid, $\nu$ is the kinematic viscosity of the fluid. Note that we can write $\mathrm{Re}_m=\mathrm{Re}\,\sigma\nu\mu_0$. If we consider mercury at temperature 30° C, then $\sigma$ has the value $10^6\,\mathrm{W}^{-1}\,\mathrm{m}^{-1}$, $\nu=1{\cdot}2\times10^{-7}\,\mathrm{m}^2/\mathrm{s}$. Given that $\mu_0=4\pi10^{-7}\mathrm{N/A}^2$, it is clear that the magnetic Reynolds is of the order $10^{-7}$ smaller than the Reynolds number of the fluid. These are typical values for many other liquid metals as well. For low-magnetic-Reynolds-number flows, it is therefore assumed that the effect of the motion of the conducting fluid has a small or neglible effect on the imposed magnetic field.

If we consider next typical values for the magnetic interaction parameter $m$, again for mercury, the density $\rho=1{\cdot}35\times10^4\,\mathrm{kg\,m}^{-3}$, and taking a rotation speed of 10 revolutions per second, give $m=1{\cdot}85$ for a magnetic field strength $B_0=0{\cdot}5\,\mathrm{Tesla}$. In general, the interaction parameter $m$ takes $O(1)$ values for modest rotation speeds and magnetic field values. This means that the effect of the magnetic field on the fluid motion represented by the Lorentz force term $m\mathbf{J}\times\mathbf{B}$ in the fluid equations cannot be neglected.

The fluid equations can be written in component form as

$$\frac{\partial u}{\partial t}+u\frac{\partial u}{\partial r}+\frac{v}{r}\frac{\partial u}{\partial\theta}+w\frac{\partial u}{\partial z}-\frac{v^2}{r}-2v-r=-\frac{\partial P}{\partial r}+\frac{1}{R^2}\left[\nabla^2 u-\frac{2}{r^2}\frac{\partial v}{\partial\theta}-\frac{u}{r^2}\right]+mL_1, \tag{2a}$$

$$\frac{\partial v}{\partial t}+u\frac{\partial v}{\partial r}+\frac{v}{r}\frac{\partial v}{\partial\theta}+w\frac{\partial v}{\partial z}+\frac{uv}{r}+2u=-\frac{1}{r}\frac{\partial P}{\partial\theta}+\frac{1}{R^2}\left[\nabla^2 v+\frac{2}{r^2}\frac{\partial u}{\partial\theta}-\frac{v}{r^2}\right]+mL_2, \tag{2b}$$

$$\frac{\partial w}{\partial t}+u\frac{\partial w}{\partial r}+\frac{v}{r}\frac{\partial w}{\partial\theta}+w\frac{\partial w}{\partial z}=-\frac{\partial P}{\partial z}+\frac{1}{R^2}[\nabla^2 w]+mL_3, \tag{2c}$$

$$\frac{\partial u}{\partial r}+\frac{1}{r}\frac{\partial v}{\partial\theta}+\frac{\partial w}{\partial z}+\frac{u}{r}=0, \tag{2d}$$

where $(L_1, L_2, L_3)=(\mathbf{E}+\mathbf{u}\times\mathbf{B})\times\mathbf{B}$ are the components of the Lorentz force.

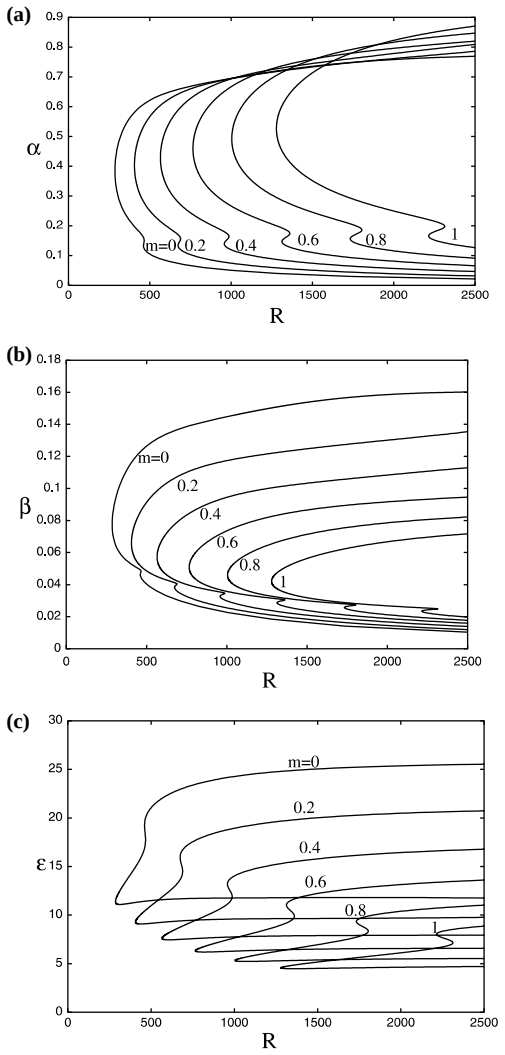


*Figure 4.* Neutral-stability curves in the (a) $(R, \alpha)$, (b) $(R, \beta)$, and (c) $(R, \varepsilon)$, planes for stationary waves ($\omega = 0$) and various magnetic-field strengths $m$.

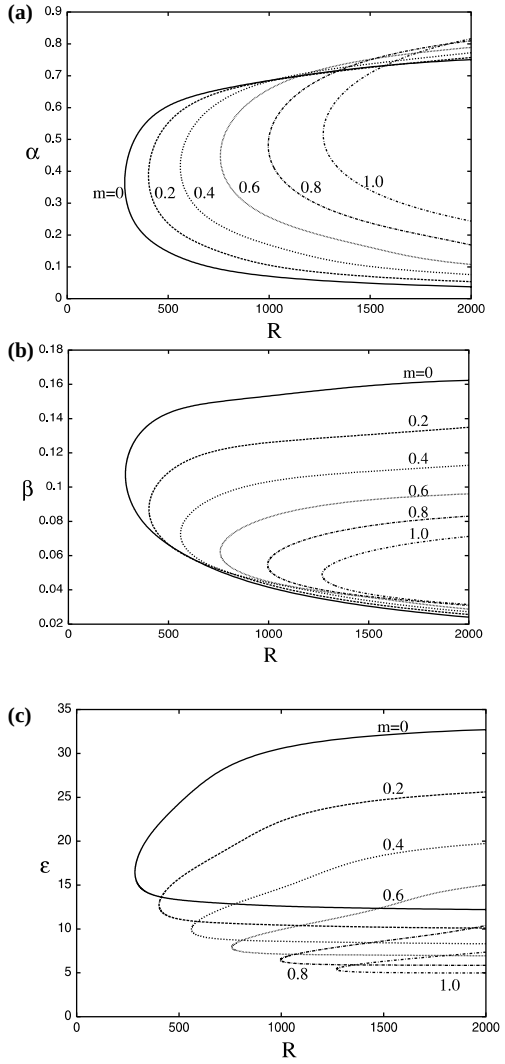


*Figure 5.* Neutral-stability curves in the (a) $(R, \alpha)$ and (b) $(R, \beta)$ representing wave numbers and (c) $(R, \varepsilon)$ wave angle planes for $\omega = -5$ and various magnetic-field strengths $m$.

Here, we have a global Reynolds number $\mathrm{Re} = R^2$, where $R$ is the Reynolds number based on the displacement thickness $\delta = (\nu/\Omega)^{\frac{1}{2}}$. The Laplacian operator in cylindrical coordinates is

$$\nabla^2 = \left( \frac{\partial^2}{\partial r^2} + \frac{1}{r^2}\frac{\partial^2}{\partial \theta^2} + \frac{\partial^2}{\partial z^2} + \frac{1}{r}\frac{\partial}{\partial r} \right).$$

Throughout this analysis, the fluid is assumed to lie in the semi-infinite space $z \geq 0$.

### 2.2. The mean-flow equations

A self-similar solution is sought for the mean flow velocity. The boundary-layer coordinate $Z$, which is of order $O(1)$, is defined as $Z = zR$. The self-similar form for the mean-flow

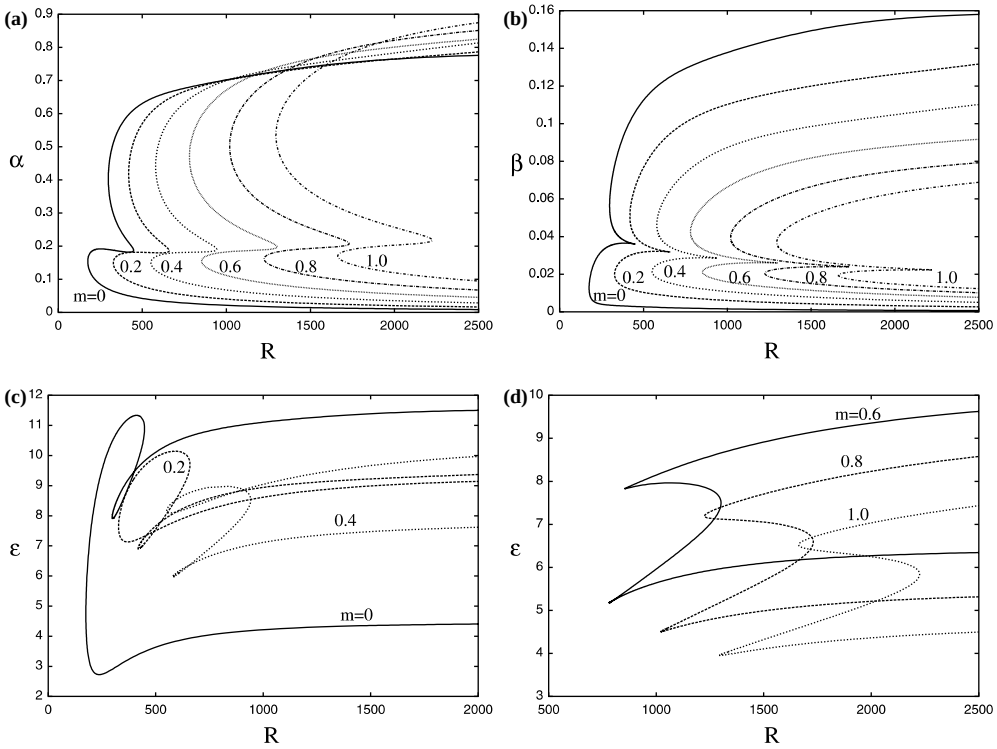


*Figure 6.* Neutral-stability curves in the (a) $(R, \alpha)$, (b) $(R, \beta)$, and (c, d) $(R, \varepsilon)$ planes for $\omega = 4$ and different magnetic-field strengths $m$.

quantites (with a suffix **B** denoting a mean-flow quantity), take the form:

$$(u, v, w, p) = (u_B, v_B, w_B, p_B) = [rF(Z), rG(Z), \frac{1}{R}H(Z), \frac{1}{R^2}P(Z)]. \tag{3a}$$

In addition the magnetic field and electric fields are expressed as

$$\mathbf{B} = \mathbf{k}, \quad \mathbf{E} = (0, 0, E_3(z)), \tag{3b}$$

where $\partial E_3/\partial Z = -2G(Z)/R$ ensures that the divergence of **J** equals zero and also that $\nabla \times \mathbf{E} = 0$. This gives

$$(L_1, L_2, L_3) = (-rF(Z), -rG(Z), 0).$$

By taking the electric field to be in the $z$-direction only, we are assuming that there are no radial currents set-up both for the mean and perturbed flow. Radial currents can be incorporated into the analysis by taking a non-zero radial component of the electric field, but this leads to slightly modified mean flow equations with an additional parameter, see Stephenson [11].

Substitution in the Navier-Stokes equations gives rise to the self-similar equations

$$F^2 - (G+1)^2 + F'H - F'' + mF = 0, \tag{4a}$$

$$2F(G+1) + G'H - G'' + m(G+1) = 0, \tag{4b}$$

$$P' + H'H - H'' = 0, \tag{4c}$$

$$2F + H' = 0, \tag{4d}$$

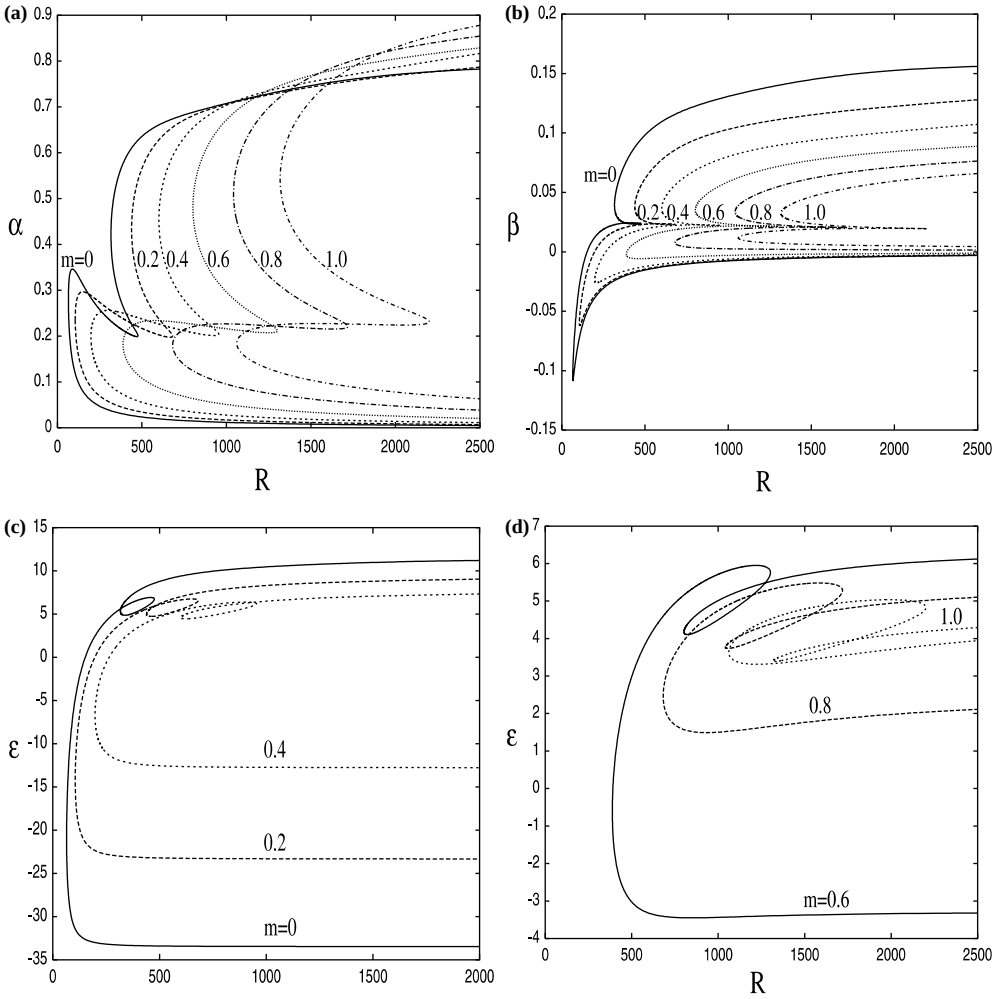


*Figure 7.* Neutral-stability curves in the (a) $(R, \alpha)$, (b) $(R, \beta)$, and (c, d) $(R, \varepsilon)$ planes for $\omega = 7{\cdot}9$ and different magnetic-field strengths $m$.

where $m = \sigma B_0^2/\rho\Omega$ is the magnetic interaction parameter assumed to be a constant. Here, primes denote derivatives with respect to $Z$. The appropriate boundary conditions are

$$F = G = H = 0 \quad \text{at} \quad Z = 0, \tag{5a}$$

$$F = 0, \quad G = -1, \quad \text{as} \quad Z \to \infty. \tag{5b}$$

The equations for the mean flow are similar to those formulated by Sparrow and Cess [10], Thacker *et al.* [12], and Hossain *et al.* [13] for a rotating-disk flow when subjected to a uniform magnetic field imposed normal to the disk.

It can be shown that the equations imply that $H \to h_\infty$ where the value of $h_\infty$ is a constant vertical velocity of the rotating fluid in the far field above the disk, and it has to be found numerically in the course of the solution of Equations (4) and (5). The Equations (4) with $m = 0$ reduce to Von-Kármán's [1] equations in the non-magnetic case.

### 2.3. Linear stability equations

Next consider infinitesimal perturbations to Von-Kármán's self-similarity velocity profiles (4). The instantaneous non-dimensionalized velocity components imposed on the basic steady flow

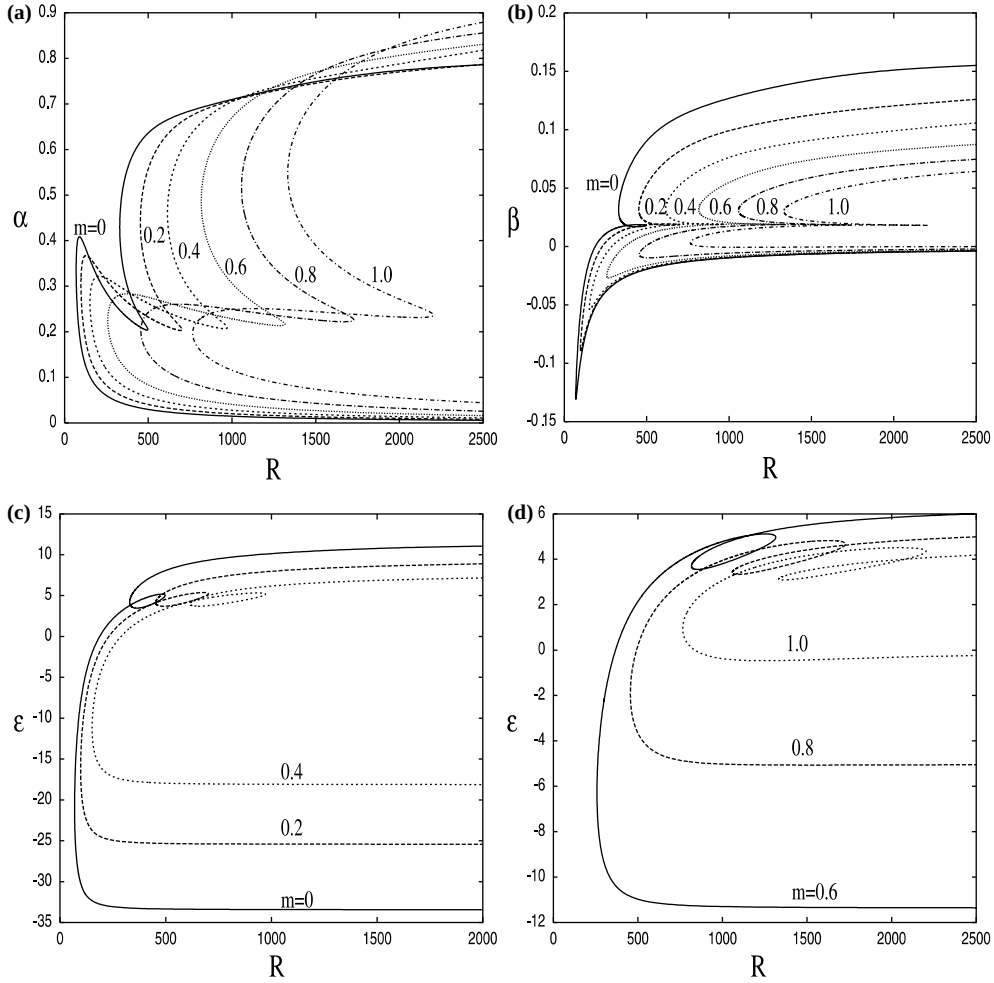


*Figure 8.* Neutral-stability curves in the (a) $(R, \alpha)$, (b) $(R, \beta)$, and (c, d) $(R, \varepsilon)$ planes for $\omega = 10$ and different magnetic-field strengths $m$.

$u$, $v$, $w$, and the pressure component $p$ can be expressed as

$$u(r,\theta,z,t) = u_B + u'(r,\theta,z,t), \quad v(r,\theta,z,t) = v_B + v'(r,\theta,z,t),$$
$$w(r,\theta,z,t) = w_B + w'(r,\theta,z,t), \quad p(r,\theta,z,t) = p_B + p'(r,\theta,z,t).$$

The disturbance components of the above system are determined by solving the form of the Navier-Stokes equations that result from substituting these quantities in (2), and subtracting off the mean-flow equations. We linearize the equations for small perturbations. We find that the linearized Navier-Stokes operator has coefficients independent of $\theta$ and hence the disturbances can be decomposed into a normal mode form proportional to $\mathrm{e}^{\mathrm{i}R(\beta\theta-\omega t)}$. Such an approximation leads the disturbances to be wave-like, separable in $\theta$ and $t$. Consequently, the perturbations may be assumed to be of the form

$$(u', v', w', p') = (\widetilde{u}[r, Z], \widetilde{v}[r, Z], \widetilde{w}[r, Z], \widetilde{p}[r, Z])\mathrm{e}^{\mathrm{i}R(\beta\theta-\omega t)} + \text{c.c.},$$

where $\beta$ represents the wave number in the azimuthal direction, $\omega$ the scaled frequency of the wave propagating in the disturbance wave direction, and c.c. denotes the complex conjugate.

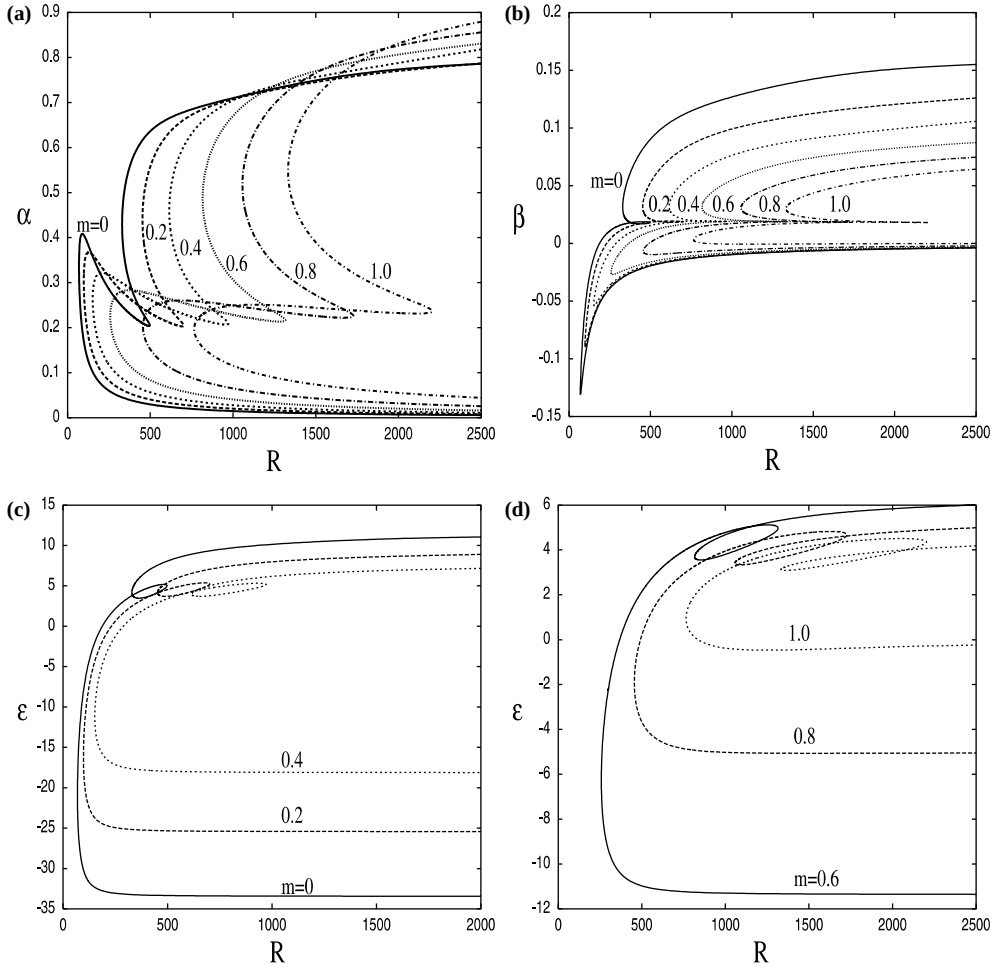


*Figure 9.* Neutral-stability curves in the (a) $(R,\alpha)$, (b) $(R,\beta)$, and (c, d) $(R,\varepsilon)$ for $\omega=10$ and different magnetic-field strengths $m$.

The separation in $\theta$ and $t$ simplifies the linear system of equations. However, no such simplification arises as far as the $r$-dependence is concerned (except in the limit for $R\to\infty$). The full linearized partial differential system has to be solved subject to suitable initial conditions to determine the stability of the flow. By introducing a suitable parallel-flow approximation – see [6] and [14] for more details – we obtain the reduced sixth-order linear system of equations. By replacing $\tilde{u},\tilde{v},\tilde{w}$, and $\tilde{p}$, by $f$, $g$, $h$, and $p$, respectively, we have

$$f''-Hf'-[\mathrm{i}R(\alpha F+\beta G-\bar{\omega})+\lambda^2+F+m]f+2(G+1)g-RF'h-\mathrm{i}\alpha Rp=0, \tag{6a}$$

$$g''-Hg'-[\mathrm{i}R(\alpha F+\beta G-\bar{\omega})+\lambda^2+F+m]g-2(G+1)f-RG'h-\mathrm{i}\beta Rp=0, \tag{6b}$$

$$h''-Hh'-[\mathrm{i}R(\alpha F+\beta G-\bar{\omega})+\lambda^2+H']h-Rp'=0, \tag{6c}$$

$$\bar{\alpha}f+\mathrm{i}\beta g+h'=0, \tag{6d}$$

where $\alpha$ is the spatial wave-number, $\bar{\omega}=\omega/R$, $\lambda^2=\alpha^2+\beta^2$, $\bar{\alpha}=\mathrm{i}\alpha+R^{-1}$. For the non-magnetic case, the linear equation system above is identical to the one used by previous investigators, such as Malik [15].

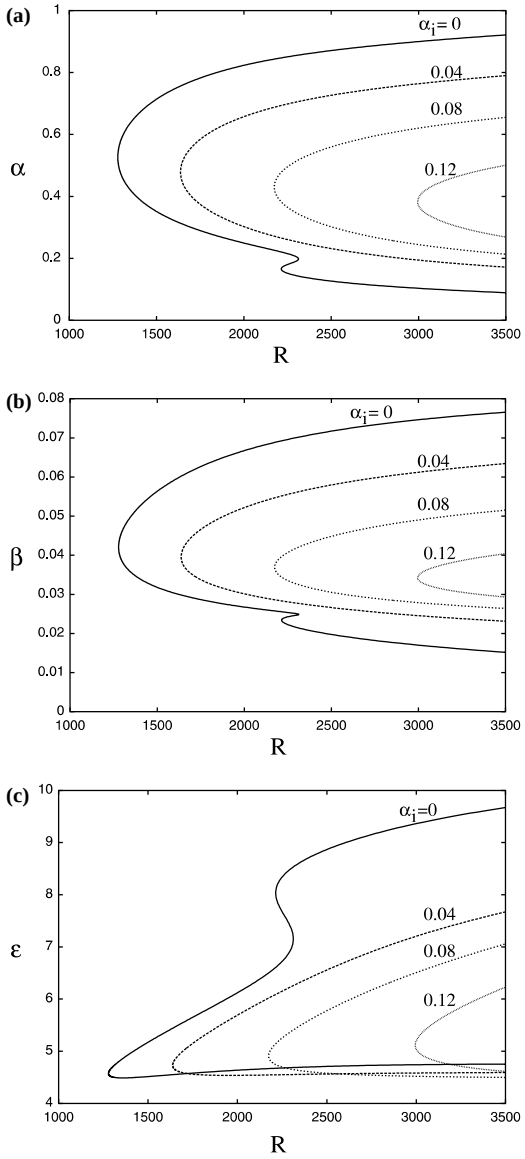


*Figure 10.* Stability curves showing contours of growth rates in the (a) $(R, \alpha)$, (b) $(R, \beta)$, and (c) $(R, \varepsilon)$ for $\omega = 0$ and $m = 1$.

The boundary conditions for this set of equations are $f = g = h = 0$ at the solid wall $(Z = 0)$ together with decay of disturbance at $Z = \infty$.

## 3. Solution of the linear equations

Several methods are available for solving the linearized stability equations. In our study we solve this system of equations by using the same spectral method as in [5] but also include arclength continuation. The spectral approximation is based on Chebyshev collocation with a staggered grid for the pressure terms in the normal direction. For a fuller description of the method, see [6]. When Newton's method fails to converge at a turning point, we use in

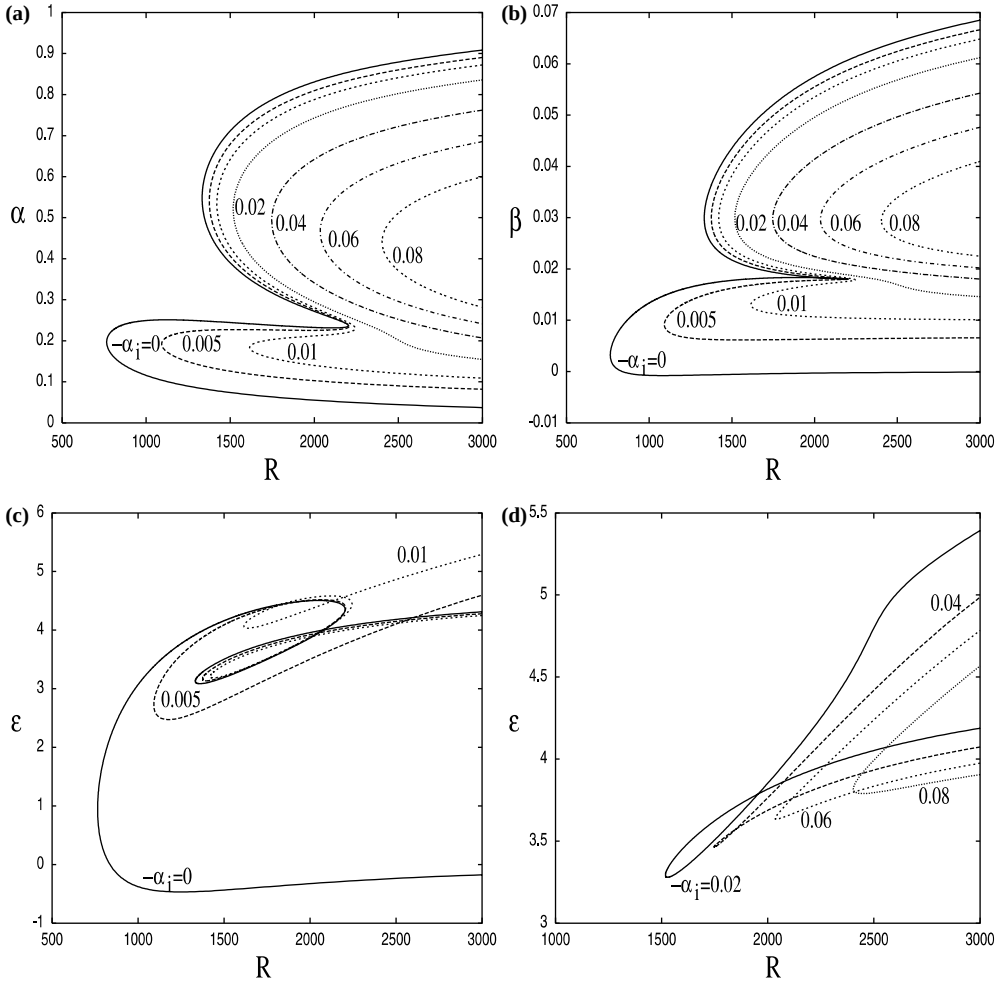


*Figure 11.* Stability curves showing growth rates in the (a) $(R, \alpha)$, (b) $(R, \beta)$, and (c, d) $(R, \varepsilon)$ for $\omega = 10$ and $m = 1$.

addition the arclength continuation method. Thus, we encounter no difficulties at a limit point or at a vertical inflection point.

### 3.1. Solution of the mean flow

The mean flow Equations (4) are solved using a finite-difference method employing the Numerical Algorithms Group (NAG) routine D02RAF. The corresponding normal velocity $h_\infty$ is then evaluated. In Figure 2 we show plots of the similarity profiles $F(Z), G(Z), H(Z)$ *vs.* $Z$ for different values of $m$. The results clearly demonstrate that increasing $m$ leads to a reduction in the magnitude of the mean velocity as compared to the non-magnetic case for fixed $Z$.

For large $m$, the Equations (4) and (5) can be solved analytically, as in [10]. We expand the basic velocity components as

$$F = m^{-1} F_0(\bar{z}) + \cdots, \quad G = G_0(\bar{z}) + \cdots, \quad H = m^{-3/2} H_0(\bar{z}) + \cdots, \tag{7a,b,c}$$

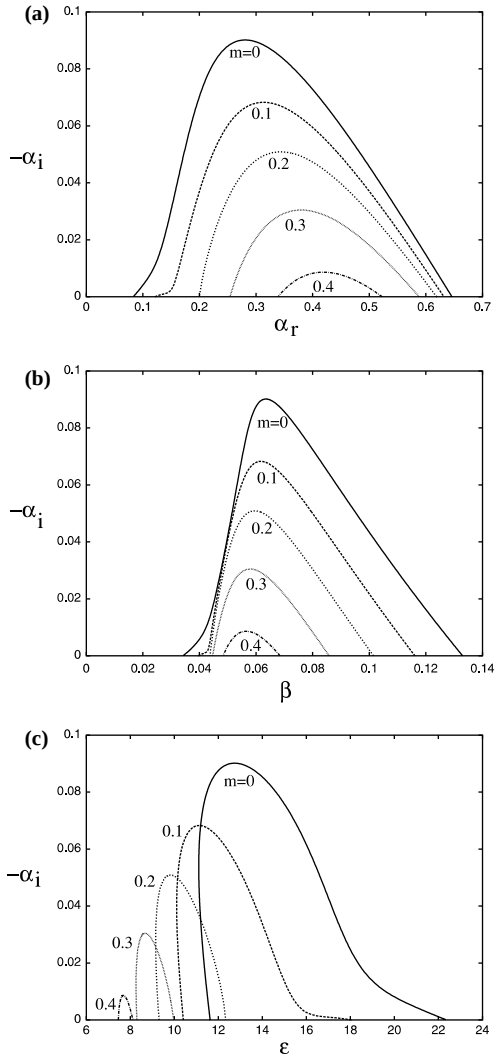


*Figure 12.* Spatial amplication rates for zero-frequency waves as a function of wave numbers (a) $(\alpha_i, \alpha_r)$, (b) $(\alpha_i, \beta)$, and wave angle (c) $(\alpha_i, \varepsilon)$ for $R$ = 600 and different values of $m$.

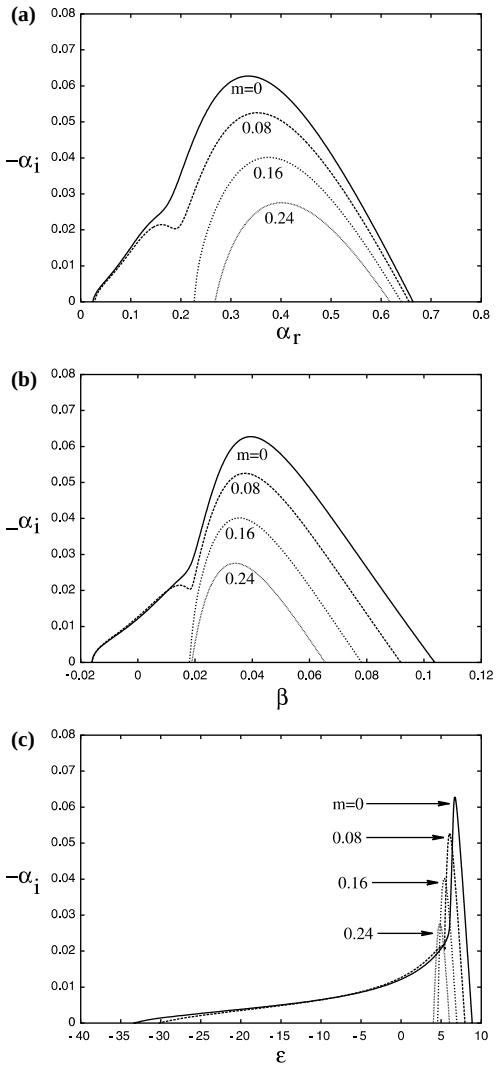


*Figure 13.* Spatial amplication rates of travelling waves with a frequency of $\omega = 10$ as a function of wave numbers (a) $(\alpha_i, \alpha_r)$, (b) $(\alpha_i, \beta)$, and wave angle (c) $(\alpha_i, \varepsilon)$ for $R = 600$ and different values of $m$.

where $\bar{z} = m^{1/2} Z$. Substituing the above expansions in the Equations (4) and equating terms of order one, we obtain

$$(G_0 + 1) - G_0'' = 0, \quad F_0 - (G_0 + 1)^2 - F_0'' = 0, \quad 2F_0 + H_0' = 0.$$

The solution of this system is

$$F_0 = \frac{1}{3}(e^{-\bar{z}} - e^{-2\bar{z}}), \quad G_0 = (e^{-\bar{z}} - 1), \quad H_0 = \frac{2}{3}(e^{-\bar{z}} + \frac{1}{2}e^{-2\bar{z}}) - \frac{1}{3}.$$

Substituting for $F_0, G_0$ and $H_0$ into Equations (7) yields

$$F = m^{-1}\left[\frac{1}{3}(e^{-\bar{z}} - e^{-2\bar{z}})\right] + \cdots, \quad G = (e^{-\bar{z}} - 1) + \cdots, \quad H = m^{-\frac{3}{2}}\left[\frac{2}{3}(e^{-\bar{z}} - e^{-2\bar{z}}) - \frac{1}{3}\right] + \cdots. \tag{8a,b,c}$$

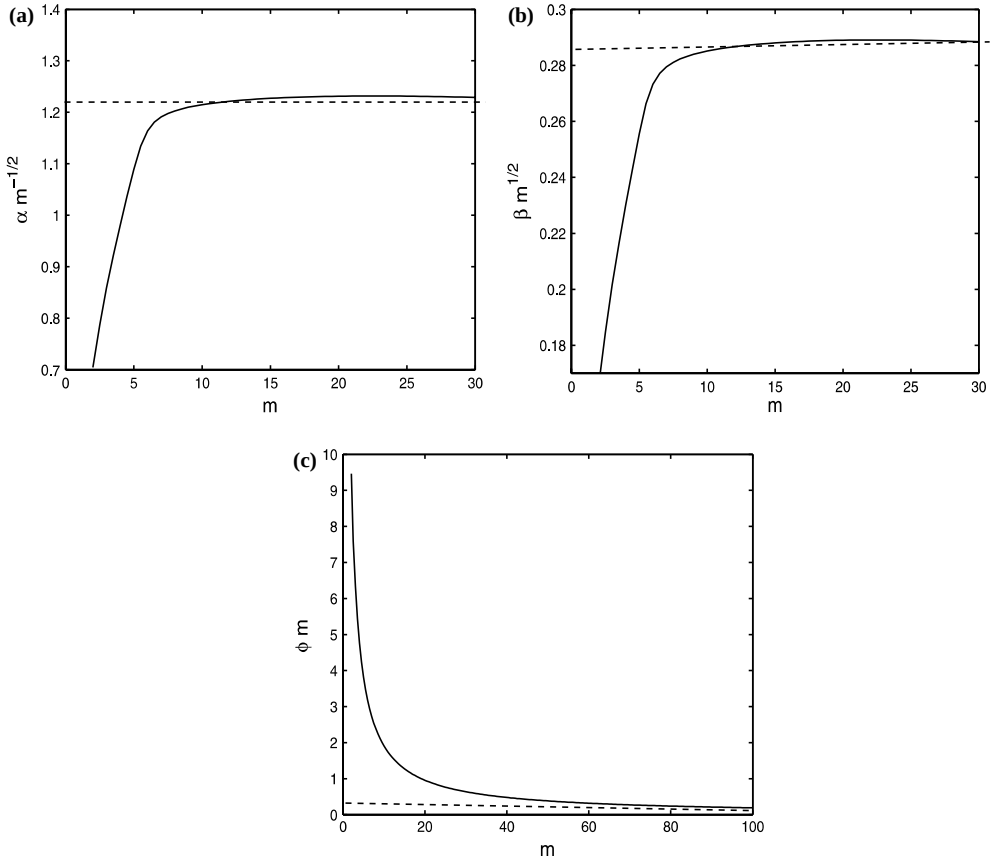


*Figure 14.* Magnetic field $m$ versus (a) $\alpha m^{-1/2}$ and (b) $\beta m^{1/2}$ and (c) $\phi m$ for $R = 1000$. The dashed line shows the asymptotic limit.

When $\bar{z} \to \infty$, this gives

$$h_\infty = -\frac{1}{3} m^{-\frac{3}{2}} \quad \text{or} \quad h_\infty m^{\frac{3}{2}} = -\frac{1}{3}. \tag{9}$$

Figure 3 exhibits a plot of $m$ *vs.* $h_\infty m^{3/2}$. It shows that, when $m$ is large, then $h_\infty m^{3/2}$ approaches the constant value $-1/3$ , which is equal to the value obtained analytically.

### 3.2. Stability results

Having discussed the properties of the mean flow, we next analyze the stability of this flow. Instability modes can be classed into two distinct types, convectively unstable modes and absolutely unstable modes. We will first discuss convective instability.

Convectively unstable modes can be further sub-divided into two classes, namely stationary waves, for which the frequency $\omega = 0$ and travelling waves for which $\omega$ is non-zero.

The wave angle $\varepsilon$ of a disturbance is defined as $\varepsilon = \tan^{-1}[\beta/\alpha_r]$. In Figure 4, we display the neutral curves for stationary disturbances in the $(R, \alpha), (R, \beta), (R, \varepsilon)$, planes for several values of $m$. These figures indicate the presence of two minimum. One minimum is located on the upper branch associated with the inviscid-type instability, whereas the other minimum lies on the lower branch related to viscous-type instability.

The data show that an increase in the magnetic-field-strength parameter leads to an increase in the values of critical Reynolds numbers. Compared to the non-magnetic case, for $m = 1$ there is almost a threefold increase in the critical Reynolds number. Figure 4(c) shows

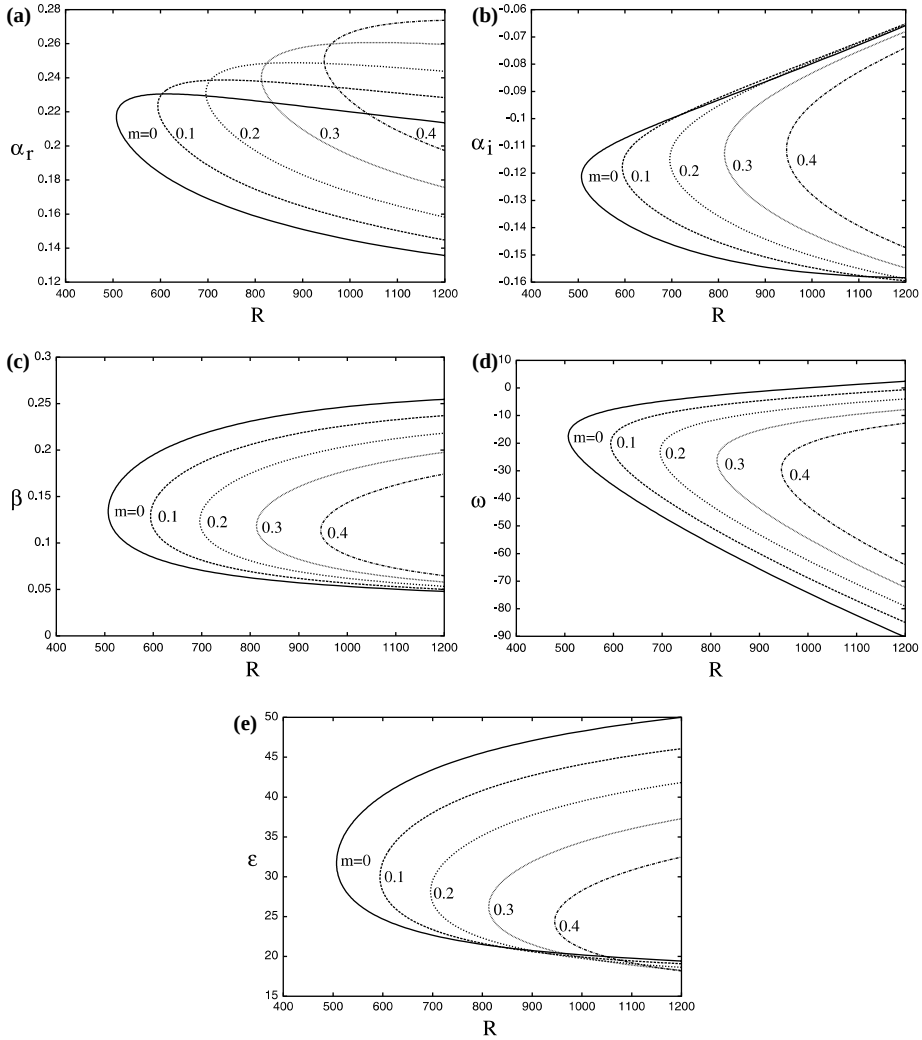


*Figure 15.* Neutral absolute instability curves in (a) $(R, \alpha_r)$, (b) $(R, \alpha_i)$, (c) $(R, \beta)$, (d) $(R, \omega)$, and $(R, \varepsilon)$ planes for different values of $m$.

that increasing $m$ causes the band of wave angles for instability to be reduced and shifted to much smaller wave angles.

Travelling waves are defined for non-zero values of the frequency $\omega$. The neutral curves for travelling waves in the $(R, \alpha)$, $(R, \beta)$, and $(R, \varepsilon)$ plans are shown in Figures (5–9) for negative as well as several positive non-dimensional frequencies and for several values of the magnetic field strength $m$. Similar curves are also shown in [5] in the absence of a magnetic field. It is noticed that a minimum occurs on the lower branch for certain frequencies. The existence of such second minima was also observed in the experiments of Faller and Kaylor [16]. They demonstrated that viscous-type as well as inviscid-type disturbances were possible in the Ekman boundary layer in the rotating-disk flow. Therefore, it was suggested that the travelling modes are more important since they have smaller critical Reynolds numbers. In the non-magnetic case the lowest critical Reynolds number occurs for a frequency $\omega = 7{\cdot}9$. For the magnetic case, this is no longer true. For instance, the critical value of the Reynolds number for $m = 1$ is 764·64 for $\omega = 10$ as compared to 1091·9 for $\omega = 7{\cdot}9$; see Figures 7 and 10. For travelling waves Figures 5–8 show that the flow is stabilized, as compared to the

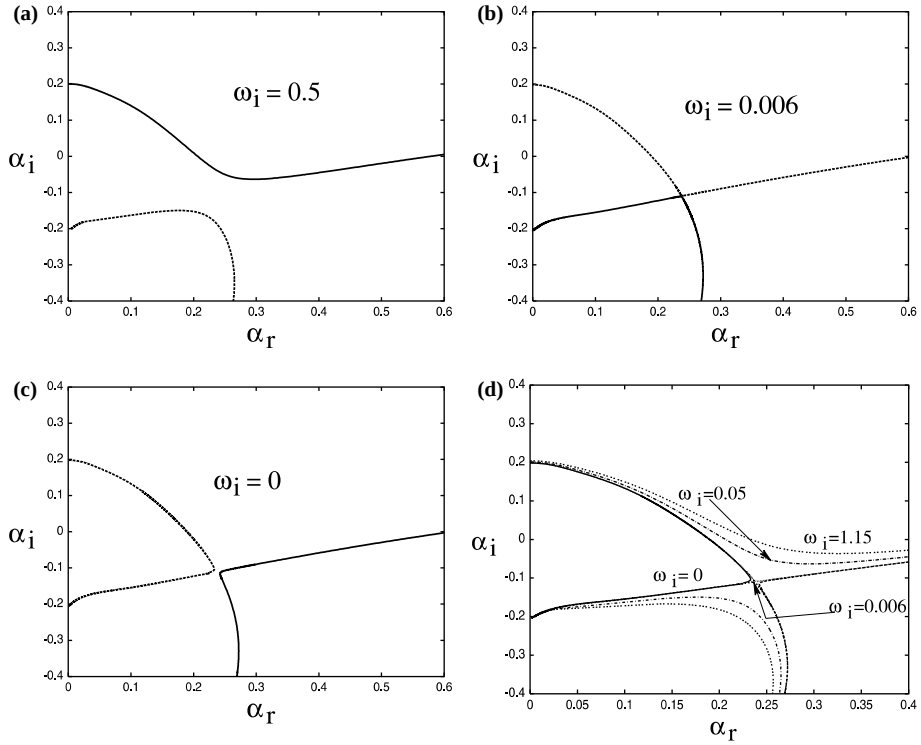


*Figure 16.* Plots showing the pinching phenomena mor $m = 0{\cdot}2$ with a branch point at $\beta = 0{\cdot}137$, $\alpha = (0{\cdot}23774, -0{\cdot}10983)$, $\omega = (-22{\cdot}66, 0{\cdot}006)$ and R = 703·83. Figures are, respectively, for (a) $\omega_i = 0{\cdot}5$, (b) $\omega_i = 0{\cdot}006$ (pinching point), and (c) $\omega_i = 0$, (d) all together.

non-magnetic case, for increasing $m$. In Figure 5 with $\omega = -5$ we observe that the lower minimum disappears from the lower branch in all the graphs. Again, for travelling waves increasing the magnetic-field parameter causes the unstable wave angles to be reduced and to be moved to smaller angles.

In Figures 10 and 11 some results for contours of growth rates for stationary and travelling waves are shown for $m = 1$. The effect of varying the field strength on the growth rate, at a fixed Reynolds number, can be seen in Figures 12 and 13. Increasing $m$ reduces the peak growth rate. The figures also demonstrate the dramatic reduction in the unstable wave angles for increasing $m$. For travelling waves the unstable negative wave angles disappear as $m$ increases; see Figure 13.

### 3.3. Some asymptotic stability properties

Following Hall [17], it is possible to derive estimates for the behaviour of the neutral wave numbers in the large-Reynolds-number limit for some special cases. In particular, for large $m$ – see Jasmine [18] for further details – it can be shown that for stationary waves on the upper-branch, the wave numbers have the expansion

$$(\alpha, \beta, c) = (\alpha_0, \beta_0, c_0) + R^{-\frac{1}{6}}(\alpha_1, \beta_1, c_1) + \cdots . \tag{10}$$

The analysis shows that

$$\frac{\beta_0}{r\alpha_0} = \frac{1}{9m}, \qquad \alpha_0 \approx \bar{\gamma} m^{\frac{1}{2}}. \tag{11}$$

Here, $\bar{\gamma}$ is $O(1)$ constant, which can be determined by solving Rayleigh's equation.

For the lower branch the wave numbers are expanded as

$$(\alpha, \beta) = (\alpha_0, \beta_0) + R^{-\frac{1}{8}}(\alpha_1, \beta_1) + \cdots . \tag{12}$$

It is found that for large $m$

$$\alpha \approx 2{\cdot}62 m^{5/4} r^{-1/2}, \quad \beta \approx 0{\cdot}78 m^{1/4} r^{1/2}, \quad \phi = \tan\hat{\epsilon} = \frac{\beta}{\alpha} = 0{\cdot}298 m^{-1} r. \tag{13a,b,c}$$

The predictions (13) are tested against the full numerical solution of the equations (6) for large $m$ at a fixed Reynolds number. Figure 14 show that the results are consistent with (13).

## 4. Absolute-instability results

Using a Newton-Raphson search procedure, we have solved the system of equations and searched for branch points of the dispersion relationship. For $m$ = 0, the eigenvalues we obtain agree with those derived earlier by Lingwood [3] and Turkyilmazoglu and Gajjar [5]. The Briggs [19, Chapter 2] criterion has been employed with fixed parameters $\beta$ and $R$ to distinguish between absolutely and convectively unstable flows.

The neutral absolute instability curves in the $(R, \alpha_r)$, $(R, \alpha_i)$, $(R, \beta)$, $(R, \omega_r)$, and $(R, \varepsilon)$ planes are shown in Figure 15 for several values of magnetic-field-strength parameter. Inside the curves, the imaginary part of the frequency $\omega$ is positive and thus the particular flow there is absolutely unstable.

For $m$ = 0, the eigenvalues we obtain agree with those derived earlier by Turkyilmazoglu and Gajjar [5]. Figure 16 shows the pinching phenomennon for $m = 0{\cdot}2$, $R = 703{\cdot}83$ and $\beta = 0{\cdot}137$. For large positive values of $\omega_i$, the branches shown lie in the distinct halves of the $\alpha$-plane. At the pinch point, $\omega_i$ is 0·006, and so this point exhibits absolute instability.

## 5. Conclusions

The stability of the flow over a rotating disk when a magnetic field normal to the disk is imposed has been investigated. The stability parameters for the stationary and non-stationary waves have been computed. Using a spectral and arclength continuation methods, stability diagrams were produced. Neutral-stability curves were sketched for various real frequencies and several values of the magnetic field strength $m$.

The major finding is that the presence of a normal magnetic field is stabilizing as compared to the non-magnetic case, for both the convective as well as the absolutely unstable modes. Increasing the magnetic strength parameter leads to increased stability. The main reason for this behaviour is that the presence of the magnetic field, seen via the Lorentz-force term, cause the mean velocities to be significantly reduced as compared to the non-magnetic case.

For large values of the magnetic-strength parameter, an analytical solution of the mean-flow equations exists and this has been used to obtain estimates for the behaviour of the eigenvalues in the stability problem in certain special cases.

In this paper, we have considered only the normal magnetic field. For a circular magnetic field the results are expected to be very different from those presented here because the mean boundary layer behaves very differently for large values of the applied field strength. In fact,

for a circular magnetic field, one would expect the flow to become more unstable with increasing value of the magnetic-strength parameter. In addition, we have considered flows which have low magnetic Reynolds numbers and neglected the influence of the fluid motion on the imposed field. Whilst this may be appropriate for many liquid metals, in plasmas the magnetic Reynolds number can assume values which are not small, and the coupled fluid magnetic interactions here can be significant and cannot be neglected.

**Acknowledgement**

Both authors would like to thank the referees for their comments which helped to improve the paper from an earlier draft.

**References**

1. T. Von-Kármán, Uber laminare und turbulente Reibung. *Z. Angew. Math. Mech.* 1 (1921) 233–252.
2. H.P Pao, Magnetohydrodynamic flows over a rotating disk. *AIAA J.* (1968) 6 1285–1291.
3. R.J. Lingwood, Absolute instability of the boundary layer on a rotating-disk. *J. Fluid Mech* (1995) 299 17–33.
4. M. Turkyilmazoglu, J.W. Cole and J.S.B. Gajjar, Absolute and convective instabilities in the compressible boundary layer on a rotating disk. *Theoret. Comput. Fluid Dyn.* 14 (2000) 21–39.
5. M. Turkyilmazoglu and J.S.B. Gajjar, Convective and absolute instability in the incompressible boundary layer on a rotating disk. CLSCM, Report No. 1998-002. University of Manchester (1998) pp. 1–61.
6. M. Turkyilmazoglu and J.S.B. Gajjar, Direct spatial resonance in the laminar boundary layer due a rotating disk. *Sadhana* 25 (2000) 601–619.
7. R.J. Lingwood, An experimental study of absolute instability of the rotating-disk boundary layer flow. *J. Fluid Mech.* 314 (1996) 373–405.
8. C. Davies and P. W. Carpenter, Global behaviour corresponding to the absolute instability of the rotating disc boundary layer. *J. Fluid Mech.* 486 (2003) 287–329.
9. B. Pier, Finite amplitude crossflow vortices secondary instability and transition in the rotating-disk boundary layer. *J. Fluid Mech.* 487 (2003) 315–343.
10. E.M. Sparrow, and R.D. Cess, Magnetohydrodynamic flow and heat transfer about a rotating disk. *ASME J. Appl. Mech.* 29 (1962) 181–187.
11. C.J. Stephenson, Magnetohydrodynamic flow between rotating coxial disks. *J. Fluid Mech.* 38 (1969) 335–352.
12. W.I. Thacker, L.T. Watson and S.K. Kumar, Magnetohydrodynamic free convection from a disk rotating in a vertical plane. *Appl. Math. Model.* 14 (1990) 527–535.
13. M.A. Hossain, A. Hossain and M. Wilson, Unsteady flow of viscous incompressible fluid with temperature-dependent viscosity due to a rotating disc in presence of transverse magnetic field and heat transfer. *Int. J. Therm. Sci.* 40 (2001) 11–20.
14. P. Balakumar and M.R. Malik, Travelling disturbances in rotating-disk flow. *Theoret. Comput. Fluid Dyn* 2 (1990) 125–137.
15. M.R. Malik, The neutral curve for stationary disturbances in rotating-disk flow. *J. Fluid Mech.* 164 (1986) 275–287.
16. A.J. Faller and R.E. Kaylor, A numerical study of the instability of the laminar Ekman boundary layer. *J. Atm. Sci.* 23 (1966) 466–480.
17. P. Hall, An asymptotic investigation of the stationary modes of instability of the boundary layer on a rotating-disk. *Proc. R. Soc. London* A 406 (1986) 93–106.
18. H.A. Jasmine, Absolute and convective instabilities in some rotating fluid flows. Ph.D. thesis University of Manchester (2003) 220 pp.
19. R.J. Briggs, *Electron-Stream Interaction with Plasmas*. Cambridge, Mass: MIT press (1964).